

# Selective Readout and Back-action Reduction for Wideband Acoustic Gravitational Wave Detectors

M. Bonaldi,<sup>1,\*</sup> M. Cerdonio,<sup>2</sup> L. Conti,<sup>2</sup> M. Pinard,<sup>3</sup> G.A. Prodi,<sup>4</sup> and J.P. Zendri<sup>5</sup>

<sup>1</sup>*Istituto di Fotonica e Nanotecnologie CNR-ITC and INFN Trento, I-38050 Povo (Trento), Italy*

<sup>2</sup>*INFN Padova Section and Department of Physics*

*University of Padova, via Marzolo 8, I-35100 Padova, Italy*

<sup>3</sup>*Laboratoire Kastler Brossel, 4 place Jussieu, F75252 Paris, France*

<sup>4</sup>*Department of Physics University of Trento and INFN Trento, I-38050 Povo (Trento), Italy*

<sup>5</sup>*INFN Padova Section, via Marzolo 8, I-35100 Padova, Italy*

We present the concept of selective readout for broadband resonant mass gravitational wave detectors. This detection scheme is capable of specifically selecting the signal from the contributions of the vibrational modes sensitive to the gravitational waves, and efficiently rejecting the contribution from non gravitationally sensitive modes. Moreover this readout, applied to a dual detector, is capable to give an effective reduction of the back-action noise within the frequency band of interest. The overall effect is a significant enhancement in the predicted sensitivity, evaluated at the standard quantum limit for a dual torus detector. A molybdenum detector, 1 m in diameter and equipped with a wide area selective readout, would reach spectral strain sensitivities  $\sim 2 \times 10^{-23} \text{ Hz}^{-1/2}$  between 2-6 kHz.

The concept of sensitive and broadband acoustic mass gravitational wave (GW) detectors has been recently presented with reference to a dual sphere detector [1]. Such a novel class of detectors may be of great interest, as they would be sensitive in a broad frequency interval of few kHz in the kHz range, were GW signals from fully relativistic stellar sources are expected [2]. A practical implementation of such a detector could suffer from: i) unwanted non-GW active resonant modes in the frequency region of interest, ii) additional thermal noise, due to the low frequency contribution of the high frequency non GW sensitive modes [3]. These difficulties may be overcome by introducing a *geometrically selective* readout, capable of specifically selecting the contribution to the signal from all the GW sensitive modes. We have found also an additional bonus: the scheme is capable to give an effective reduction of the back-action noise within the bandwidth. The overall effect is a significant enhancement in the sensitivity.

In a “dual” detector one would measure the differential displacement, driven by the GW, of the nearly faced surfaces of two concentric massive bodies, mechanically resonating at different frequencies [1]. In this scheme the centers of mass of the two bodies coincide and then remain

mutually at rest while the masses resonate. The differential displacement is then only due to the internal vibrational modes, while the centers of mass provide the rest frame for the measurement. This design allows the use of wide bandwidth (non resonant) readouts, evolution in concept and in technology of the resonant readouts used for bar detectors [4].

A basic dual detector can be represented as a simple one dimensional system [Fig. 1(a)], where a force  $F_e$ , acting on two different mechanical resonators, is evaluated by a differential measurement of their positions  $x_1$  and  $x_2$ . In the frequency region between the two resonant frequencies,  $F_e$  drives the slow resonator above its resonance  $\nu_s$  and the fast one below its resonance  $\nu_f$ . The responses of the two resonators are then out of phase by  $\pi$  radians and therefore the differential motion  $x_d$  results in a signal enhancement over the single oscillator responses [Fig. 1(b)], as shown by the transfer function  $H_{F_e} = x_d/F_e$  [Fig. 1(c)].

Such a scheme in addition leads to a reduction of the back-action noise, just within the detector bandwidth of interest. In fact the system response to the back-action force, that it is coherently applied with *opposite* direction on the two masses, is nearly exactly in phase and the consequent differential displacement is highly depressed at a frequency  $f^{**}$ , as shown in the transfer function  $H_{ba} = x_d/F_{ba}$  (Fig. 1c). We measure  $x_d$  with a displacement amplifier, described by its additive displacement and back-action force noises, with white power spectra  $S_{XX}(\omega) = S_{xx}$  and  $S_{FF}(\omega) = S_{ff}$ , so that the total displacement noise is  $S_{xx} + |H_{ba}(\omega)|^2 S_{ff}$ . The noise power spectrum on the measurement of  $F_e$ , due to the amplifier system, is then:

$$S_{F_e}(\omega) = (S_{xx} + |H_{ba}(\omega)|^2 S_{ff}) / |H_{F_e}(\omega)|^2. \quad (1)$$

If we take as reference an operation at the Standard Quantum Limit (SQL), we may consider  $S_{xx}S_{ff} = \frac{\hbar^2}{4}$ , and the noise figure can be optimized by adjusting the ratio  $S_{xx}/S_{ff}$ . In a wide bandwidth detection strategy  $S_{xx}$  and  $S_{ff}$  must be balanced to give the lowest noise within the bandwidth. In doing so we profit by the subtraction effect in the back-action noise transfer function  $H_{ba}$ , and obtain a dip at the frequency  $f^{**}$ , as shown in Fig. 1(d). We finally notice that, to fully exploit the back-action reduction features,  $f^{**}$  should be placed, by a proper choice of the system parameters, amid the oscillator frequencies.

In the case of a three-dimensional body, the dynamics of elastic deformations is given as the superposition of the dynamics of an almost infinite number of normal modes of vibration [5]. An obvious way to preserve the convenient features for signal and back action noise outlined above, is to bring the real system to be as close as possible to the idealized two modes system. In fact when only the first quadrupolar mode can be considered for each body, the response to a GW of such

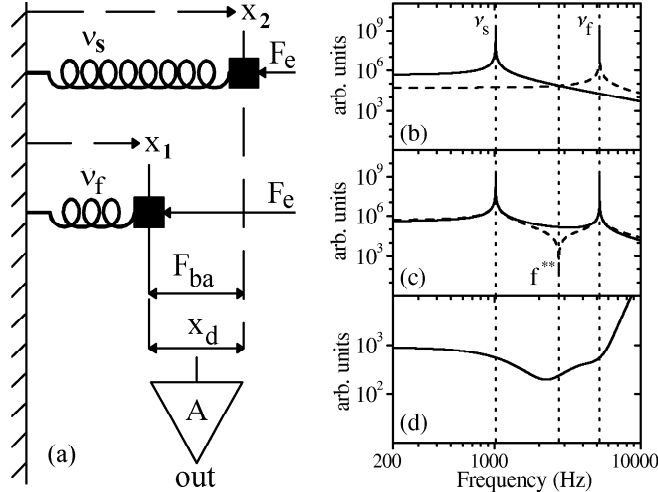


FIG. 1: (a) One-dimensional “dual” detector: the same force  $F_e$  is measured by the relative displacement  $x_d$  of two resonators. (b) Transfer functions of the slow resonator (continuous line) and of the fast resonator (dashed line). (c) Dual detector transfer functions: signal  $H_{F_e} = x_d/F_e$  (continuous line), back-action  $H_{ba} = x_d/F_{ba}$  (dashed line). (d) Wideband optimized noise.

a system can again be described by the simple one-dimensional model. This can be accomplished with a novel selective readout we propose here, capable of rejecting a large number of normal modes on the basis of their symmetry. This *geometrically based mode selection* senses the surface position of a body on specific regions, so that the related deformations can be combined with a weight/sign properly chosen to optimize the total response to normal modes of quadrupolar symmetry. Such a strategy to select specific vibrational modes and to reject a class of unwanted modes is conceptually different from the strategy now employed in GW acoustic detectors. Resonant bar detectors [6] and spherical detectors [7, 8] reconstruct the amplitude of the normal modes excited by the GWs by the use of resonant displacement readouts coupled to the modes. With a proper choice of the read-out surfaces, the resonant scheme is not sensitive to the thermal noise of out of resonance modes and gives an efficient *frequency based mode selection*. However this feature necessarily limits the detector bandwidth, due to the thermal noise contribution of the resonant transducer, as in every resonant readout scheme. By contrast the *geometrically based mode selection* selects gravitationally sensitive normal modes by means of their geometrical characteristics, and shows a significant rejection of non quadrupolar modes without affecting the detector bandwidth. For this reason it can be effectively applied to a “dual” wideband detector.

Without loss of generality, we apply these new concepts to a dual torus detector [Fig. 2(a)], a convenient geometry where the advantages of the proposed scheme can be fully exploited. In the

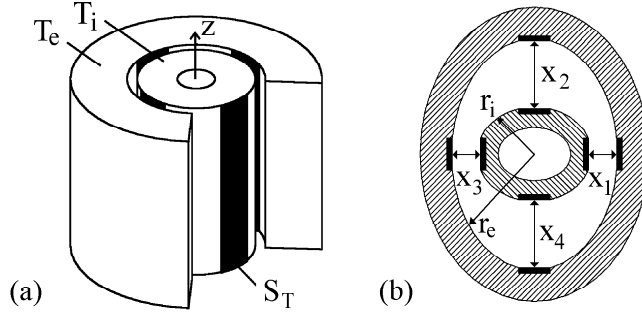


FIG. 2: (a) The two concentric torii,  $T_e$ ,  $T_i$  are made of materials of density  $\rho_e$ ,  $\rho_i$  and have the same height. The inner torus may also have null internal radius and be reduced to a cylinder. The relative distance between the two bodies is measured in 4 regions (in black), each of area  $S_T$ , for the whole torus height. (b) Section of the detector showing the signal enhancement obtained when a GW signal drives the external torus above resonance and the internal torus below resonance. The difference  $X_d = x_1 + x_3 - x_2 - x_4$ , proportional to the GW strength, is not dependent on a number of non GW sensitive modes.

dual torus we average the differential displacement in 4 distinct areas  $x_{1..4}$  [Fig. 2(b)] and combine them to obtain  $X_d = x_1 + x_3 - x_2 - x_4$ . The detector displays its maximal sensitivity when the GW propagates along the  $z$  axis, the symmetry axis of the system. The corresponding force does not depend on  $z$  and the system response can be well described by plane strain solutions, where the displacements are functions of  $x$  and  $y$  only and the displacement along  $z$  vanishes. All the components of the internal stress are also independent by  $z$ . In this case the displacement normal modes of a single torus, eigenfunctions of the free body dynamic equations, are functions of the kind:

$$\begin{aligned} \mathbf{w}_{a,n}^+(\mathbf{r}) &= f_{a,n} \cos(a\theta) \mathbf{i}_r + g_{a,n} \sin(a\theta) \mathbf{i}_\theta \\ \mathbf{w}_{a,n}^\times(\mathbf{r}) &= -f_{a,n} \sin(a\theta) \mathbf{i}_r + g_{a,n} \cos(a\theta) \mathbf{i}_\theta, \end{aligned}$$

where the functions  $f_{a,n}, g_{a,n}$  are linear combinations of Bessel functions of the coordinate  $r$ , with coefficients given by the boundary conditions. The integer  $a$  represents the angular symmetry of the mode, while  $n$  identifies the mode order within the angular family. The orthogonal displacement fields  $\mathbf{w}_{a,n}^+, \mathbf{w}_{a,n}^\times$  represent the same radial distribution of the deformation, mutually rotated by  $\frac{\pi}{2a}$ : for this reason they share the same eigenvalue  $\omega_{a,n}$ , called resonant frequency of the mode. Any displacement  $\mathbf{u}$  may be written as linear superposition of these basis functions:

$$\mathbf{u}(\mathbf{r}, t) = \sum_{s, a, n} \mathbf{w}_{a,n}^s(\mathbf{r}) q_{a,n}^s(t), \quad (2)$$

where the time dependent coefficients are determined by the force acting on the body and  $s = +, \times$ .

A + polarized GW propagating along the  $z$ -axis applies on the mass of density  $\rho$  the force density  $F_{gw}(t) \mathbf{G}_{gw}(\mathbf{r})$ :

$$\begin{aligned} F_{gw}(t) &= \frac{1}{2} \rho \ddot{h}(t) \\ \mathbf{G}_{gw}(\mathbf{r}) &= r \cos(2\theta) \mathbf{i}_r - r \sin(2\theta) \mathbf{i}_\theta. \end{aligned} \quad (3)$$

For symmetry reasons this force can only excite  $\mathbf{w}^+$  quadrupolar ( $a = 2$ ) modes. A “weight function” approach to the problem will give the mathematical framework to study the selective read-out, which implements the difference  $X_d = x_1 + x_3 - x_2 - x_4$  [Fig. 2(b)]. If  $\mathbf{u}_e$  and  $\mathbf{u}_i$  are the displacements of the torus  $T_e$  and  $T_i$  [9], we define the observable physical quantity of the system as:

$$X_d(t) = \int [\mathbf{u}_e(\mathbf{r}, t) + \mathbf{u}_i(\mathbf{r}, t)] \cdot \frac{\mathbf{P}_4(\mathbf{r})}{P_N} dV, \quad (4)$$

where the “selective” measurement strategy and detection scheme is implemented by the weight function  $\mathbf{P}_4(\mathbf{r}) = P_4^r(r) P_4^\theta(\theta) \mathbf{i}_r$ , where:

$$\begin{aligned} P_4^r &= \delta(r - r_e) - \delta(r - r_i) \\ P_4^\theta &= \sum_{m=0}^1 \sum_{n=0}^4 (-1)^{n+m} \Theta[\theta + (-1)^m \alpha - n \frac{\pi}{2}] \end{aligned} \quad (5)$$

and  $\Theta(x)$  represents the unit step function. The normalization is  $P_N = S_T$ , area of one sampling region [Fig. 2(a)]. Here the term  $P_4^r$  gives the requested displacement difference  $r_e - r_i$  [Fig. 2(b)], while  $P_4^\theta$  reduces the angular integral over 4 distinct regions,  $2\alpha$  wide, centered around  $\theta = 0, \frac{\pi}{2}, \pi, \frac{3\pi}{2}$  [Fig. 3(a)]. A value  $\alpha = 0.3$  rad is assumed to perform the following calculations. For comparison we consider a non selective transducer system, which senses the displacement over a single area, centered for example at  $\theta = 0$ . Its weight function  $\mathbf{P}_1$  has angular component  $P_1^\theta = \Theta(\theta + \alpha) - \Theta(\theta - \alpha) + \Theta(\theta + \alpha - 2\pi) - \Theta(\theta - \alpha - 2\pi)$ , while the radial dependence and the normalization remain the same as  $\mathbf{P}_4$ .

When we evaluate the observable Eq. (4), by using the expansion Eq. (2) and the weight functions  $\mathbf{P}_4$  or  $\mathbf{P}_1$ , each  $\mathbf{w}_{a,n}^+$  mode contribution depends on its angular symmetry  $a$ . As shown in Fig. 3(b), in both cases the modes contribution oscillates and rapidly decreases, due to the averaging over the area  $S_T$ . But in the case of  $\mathbf{P}_4$  only the symmetry values  $a = 2 + 4k$ , with  $k$  non negative integer, give non null contributions to our observable Eq. (4). To summarize, the quadrupolar modes family ( $k = 0$ ) contribution is essentially preserved, many mode families are rejected ( $a \neq 2 + 4k, k \geq 0$ ) and the residual higher order families ( $a = 2 + 4k, k > 0$ ) give a reduced contribution.

We point out that the normal modes  $\mathbf{w}^\times$ , proportional to  $\sin(a\theta)$ , and excited by  $\times$ -polarized gravitational waves, are rejected by  $\mathbf{P}_4(\mathbf{r})$ , for every value of  $a$ . When a second transducer system, identical but rotated by  $\pi/4$ , is employed to detect these  $\mathbf{w}^\times$  modes, any  $z$ -axis propagating GW can be fully characterized in terms of intensity and polarization.

The detector sensitivity can be evaluated by the transfer function  $T_{X_d} \equiv \tilde{X}_d(\omega)/\tilde{F}(\omega)$ , which gives the observable  $X_d$  induced by a generic driving force density  $F(t)\mathbf{G}(\mathbf{r})$  [10]. We call  $(\mathbf{w}_{a,n}^s, \omega_{a,n})$  and  $(\mathbf{v}_{a,n}^s, \varpi_{a,n})$  the normal modes and eigenfrequencies of the torus  $T_e$  and  $T_i$ , while the loss angles  $(\phi, \psi)$ , inversely proportional to the mode quality factor  $Q$ , describe the dissipation. We have:

$$T_{X_d}(\omega) = \sum_{s,a,n} \frac{\int \mathbf{G}(\mathbf{r}) \cdot \mathbf{w}_{a,n}^s(\mathbf{r}) dV \int \mathbf{w}_{a,n}^s(\mathbf{r}) \cdot \frac{\mathbf{P}(\mathbf{r})}{P_N} dV}{\rho_e [(\omega_{a,n}^2 - \omega^2) + i\omega_{a,n}^2 \phi_{a,n}(\omega)]} + \frac{\int \mathbf{G}(\mathbf{r}) \cdot \mathbf{v}_{a,n}^s(\mathbf{r}) dV \int \mathbf{v}_{a,n}^s(\mathbf{r}) \cdot \frac{\mathbf{P}(\mathbf{r})}{P_N} dV}{\rho_i [(\varpi_{a,n}^2 - \omega^2) + i\varpi_{a,n}^2 \psi_{a,n}(\omega)]} \quad (6)$$

where  $\mathbf{P}(\mathbf{r})$  can be  $\mathbf{P}_4(\mathbf{r})$  or  $\mathbf{P}_1(\mathbf{r})$ . If  $F(t)$  and  $\mathbf{G}(\mathbf{r})$  are given by Eq. (3), by Eq. (6) we calculate the system transfer function to a GW, defined as  $H_{gw}(\omega) \equiv \tilde{X}_d(\omega)/\tilde{h}(\omega)$ . In the simple case  $\rho_e = \rho_i = \rho$ , we have:

$$H_{gw}(\omega) = -(\rho\omega^2/2) T_{X_d}(\omega) \Big|_{\mathbf{G}(\mathbf{r})=\mathbf{G}_{gw}(\mathbf{r})}, \quad (7)$$

while the more general case is straightforward. The read-out back-action force is applied in the sensing areas with the same intensity but opposite sign for the two bodies, so that its spatial density is given by  $\frac{\mathbf{P}(\mathbf{r})}{P_N}$ . The corresponding system transfer function is then:

$$H_{ba}(\omega) \equiv T_{X_d}(\omega) \Big|_{\mathbf{G}(\mathbf{r})=\mathbf{P}(\mathbf{r})/P_N}. \quad (8)$$

In close analogy with Eq. (1), the transfer functions Eqs. 7 and 8 give the detector sensitivity to GW as:  $S_{hh}(\omega) = (S_{xx} + |H_{ba}(\omega)|^2 S_{ff})/|H_{gw}(\omega)|^2$ . In Fig. 3(c) we compare the sensitivities of a detector, evaluated for the selective readout  $\mathbf{P}_4$  and for the single area read-out  $\mathbf{P}_1$ .

The main effect of the selective readout is to cancel out both thermal and back-action noise contributions due to the non quadrupolar modes, so that a flat response is obtained in the full bandwidth of few kHz and the back action reduction feature is exploited. The detector dimensions are properly chosen to profit by the GW sensitivity of the second order quadrupolar mode of the outer torus. We also notice that the use of large read-out sensing area highly reduces the thermal noise due to the cumulative effect of all the normal modes [11]. In fact, as the shorter wavelength modes are averaged out, a very good transfer function convergence may be obtained by adding less than 100 modes.

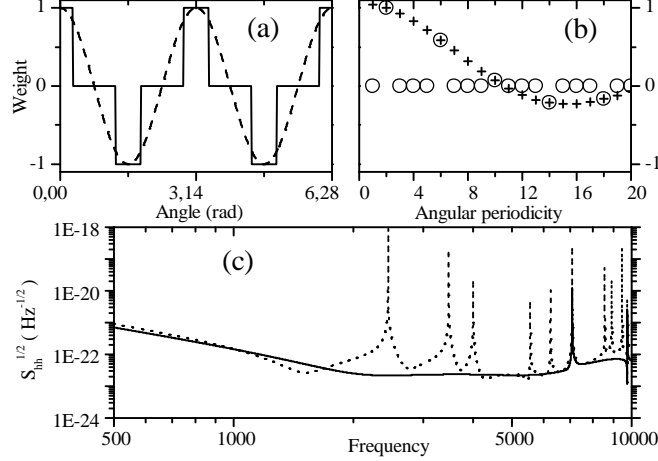


FIG. 3: (a) Angular dependence of the weight function  $\mathbf{P}_4$  (continuous line) and of the displacement induced by a  $\mathbf{w}^+$  mode (dashed line) with symmetry  $a = 2$ ; the mode contribution is proportional to the integral of the product of these two functions. (b) Normalized angular contribution of normal modes as a function of  $a$  evaluated for the weight functions  $\mathbf{P}_4$  (hollow symbols) and  $\mathbf{P}_1$  (crosses). (c) Predicted sensitivity of a Mo dual torus detector (same as Fig. 4) with the selective read-out  $\mathbf{P}_4$  (continuous line) and with the standard read-out  $\mathbf{P}_1$  (dotted line).

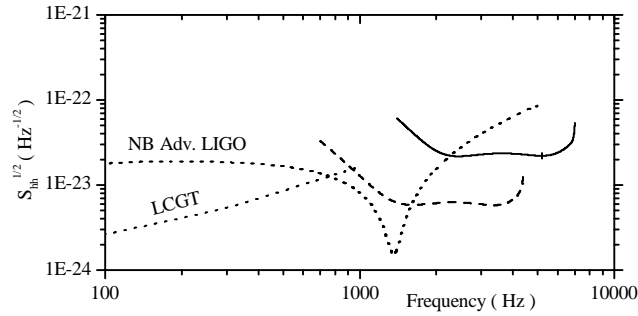


FIG. 4: Predicted spectral strain SQL sensitivities of two different dual detector configurations. The predicted SQL sensitivities of two advanced interferometric detectors are also shown (dotted lines): LCGT and a narrow band design of Advanced LIGO. Continuous line: Mo dual detector, inner cylinder radius 0.25 m, outer torus internal-external radius 0.26-0.47 m, height 2.35 m, weight 4.8 + 11.6 tons, fundamental quadrupolar modes 1012 Hz and 5189 Hz, amplifier noise  $S_{xx} = 5 \times 10^{-46} \text{ m}^2/\text{Hz}$ ,  $Q/T > 2 \times 10^8 \text{ K}^{-1}$ . Dashed line: SiC detector, inner cylinder radius 0.82 m, outer torus internal-external radius 0.83-1.44 m, height 3 m, weight 20.5 - 41.7 tons,  $S_{xx} = 3 \times 10^{-46} \text{ m}^2/\text{Hz}$ ,  $Q/T > 2 \times 10^8 \text{ K}^{-1}$ .

Finite element analysis demonstrates the selective read-out rejection capabilities also for many classes of 3-dimensional vibrational modes. The sensitivity enhancement over the standard readout scheme is then not limited to our plane strain approximation, and the dual torus configuration could be evolved in a complete detector. A practical readout configuration is a series of 4 capacitive

transducers, gradiometrically connected and sensed by a single SQUID amplifier. This implements the selective scheme  $\mathbf{P}_4$  and the consequent back-action reduction. The needed sensitivity could be reached as recent progress show that the SQUID amplifiers are approaching the quantum limit, now also in the necessary strong coupling configuration [12], and that the electric polarization field can be increased up to the material intrinsic limitations [13].

To evaluate the limits of our design, we can evaluate the sensitivity at the SQL of some practical configurations of detector material and geometry. As usual a low dissipation material is required to reduce the effect of the thermal noise. Molybdenum represents an interesting choice, as it shows high cross-section for GWs and its mechanical dissipation was investigated at low temperature giving  $Q/T > 2 \times 10^8 \text{ K}^{-1}$  for acoustic normal modes [14]. In Figs. 3 and 4 is shown the SQL sensitivity of a Mo detector with dimensions within the present technological production capabilities. In Fig. 4 we also show the SQL of a detector made of SiC, a ceramic material currently used to produce large mirrors or structures [15], with mechanical and thermal properties of interest here but not jet characterized in terms of low temperature mechanical dissipation.

The selective readout scheme applied to the dual concept allows the design of detectors tailored for relatively high frequency GW and with very few spurious modes within their wide bandwidth. These features could make the dual torus detector complementary to advanced interferometric detectors, as shown in Fig. 4 by the comparison with the expected sensitivities of LCGT [16] and one of the possible setting of Advanced LIGO in narrow band operation [17].

---

\* Corresponding author: bonaldi@science.unitn.it

- [1] M. Cerdonio, *et al.*, Phys. Rev. Lett. **87** 031101 (2001).
- [2] K. Thorne in *300 Years of Gravitation*, S.W. Hawking and W. Israel eds. (Cambridge University Press, N.Y. 1987)
- [3] L. Conti *et al.* Class. Quant. Grav. **19** 2013 (2002).
- [4] A. Marin *et al.*, Class. Quant. Grav. **19** 1991 (2002).
- [5] A.E.H. Love, *A treatise on the mathematical theory of elasticity* (Dover, New York, 1944).
- [6] Z.A. Allen *et al.*, Phys. Rev. Lett. **85**, 5046 (2000)
- [7] S.M. Merkowitz *et al.*, Phys. Rev. D **56**, 7513 (1997).
- [8] J.A. Lobo, Mon. Not. R. Astron. Soc. **316** 173 (2000).
- [9] We assume that the solutions  $\mathbf{u}_e$  and  $\mathbf{u}_i$  are independent.
- [10] In our approximation this force must be null, with its derivatives, along the  $z$ -axis. This condition is fulfilled by the considered gw force and back-action force.



- [11] A. Gillespie and F. Raab, Phys. Rev. D **52**, 577 (1995).
- [12] A. Vinante *et al.* Appl. Phys. Lett. **79**, 2597 (2001).
- [13] S. Kobayashi, IEEE Trans. on Dielect. Elec. Ins. **4**, 841 (1997).
- [14] W. Duffy, Jr., J. Appl. Phys. **72**, 5628 (1992).
- [15] B. Harnisch *et al.*, ESA bulletin **95** (1998).
- [16] K. Kuroda *et al.*, Class. Quantum Grav. **19**, 1237 (2002)
- [17] P. Fritschel in *Gravitational-Wave Detection*, P. Saulson and M. Cruise eds., Proc. SPIE **4856** (2003).